

# A BRDF Representing Method Based on Gaussian Process

Jianying Hao, Yue liu, Dongdong Weng

School of optoelectronics, Beijing Institute of Technology, 5 South Zhongguancun Street, Haidian District, Beijing, China

**Abstract.** In recent years, digital reconstruction of cultural heritage provides an effective way of protecting historical relics, in which the modeling of surface reflection of historical heritage with high fidelity places a very important role. In this paper Gaussian process (GP) regression based approach is proposed to model the reflection properties of real materials, in which the simulation data generated by the existing model are both used as the training data and the proof that Gaussian process model can be used to describe the material reflection. Matusik's MERL database is also adopted to perform training and inference and obtain the reflection model of the real material. Simulation results show that the proposed GP regression approach can achieve a good fitting of the reflection properties of certain materials, greatly reduce the BRDF measurement time and ensure high realistic rendering at the same time.

## 1 Introduction

Cultural heritage provide very important physical treasure for studying ancient history, art and development of science and technology. On one hand, the old history cultural heritage is experiencing considerable damage with the passage of time, and needs digital protection, so establishing a digital model of cultural heritage is of great essence. On the other hand, realistic digital display technology is needed to spread the cultural relic's value throughout the world. Precisely relics' digital model should include the original 3D information and correct surface texture information. At present, we can use 3D scanners, three-dimensional modeling software (such as 3DMax, Multi Creator) and many other methods to construct three-dimensional geometric models. But the complexity of reflection phenomenon and the high dimension of reflection data makes the technology of material reflection property acquisition and modeling much more difficult and has been an important research content for a long time.

The light properties on the surface of materials are determined by the interaction between light and objects. The interaction between light and surfaces can be described by a function of 12 dimensions[1]. In practice, for uniform opaque materials, ignoring the space and time changing characteristics, the reflectance function can be simplified as a 4 dimensional bidirectional reflectance distribution function (BRDF)[1]. BRDF describes the appearance of a material by its

interaction with light at a surface point and is a function of incident and observation direction vector. The BRDF is denoted symbolically as  $f$ , as shown in (1).

$$f(\theta_{in}, \varphi_{in}, \theta_{out}, \varphi_{out}) = \frac{dL_r(\theta_{in}, \varphi_{in}; \theta_{out}, \varphi_{out}; E_{in})}{dE_i(\theta_{in}, \varphi_{out})(sr^{-1})} [sr^{-1}] \quad (1)$$

A classical BRDF measurement device is gonioreflectometer[1], which samples the angular dependency sequentially by positioning a light source and a detector at various directions. Matusik et al.[2] took images from curved sample to measure isotropic BRDFs and reduced the measuring times significantly. In order to reduce the damage to the cultural relic caused by contacting and being exposed to bright light, measurement times should be reduced. Some researchers also use little measured data to fit the analytical model to represent BRDFs[4, 8, 7, 12, 5, 13]. But for complex phenomena of reflection, the performance of analysis models with a single lobe is not very good[11]. It is found that there are many extraneous information between BRDFs of different incident and output angles. In this paper, we put forward the method of using Gaussian process, which is based on Bayesian inference method, to learn the relationship between BRDFs of different angles and predict BRDFs of new angle in the whole space. Through the establishment of Gaussian model we can reduce the measurement times dramatically and get more promising rendering performance.

## 2 Related work

In order to establish material reflection model and reconstruct the cultural relics with high sense of reality, we studied different existing methods of BRDF modeling. Analytical BRDF models used for rendering can be divided into three categories: empirical (i.e., phenomenological) models, physically-based models and data-driven models. Empirical models such as Phong model[3], the Ward model[4] and anisotropic Phong model[5] etc. focus on using a specific formula to match the surface reflection effect and do not consider the physical mechanism of the light-material interaction explicitly, which makes them concise and the performance becomes idealistic. Torrance and Sparrow[6] supposed that there are many small triangle micro-facets on the material surface and used the micro-facets to describe roughness of the surface. Later, Cook[7] and Blinn[8] improved the Torrance-Sparrow model, and put forward the Cook-Torrance and Blinn model respectively.

Based on optical and electromagnetic wave theory, these physical-based models consider Fresnel effect and the micro-scale geometry of a surface so that they can describe the roughness of real material surface more effectively. Although physically-based BRDF models have a stronger theoretical basis than empirical models, fitting physically-based model parameters to measured BRDF data is not necessarily easier. Also, the surface approximate assumption can't represent the object surface reflection mechanism of different materials exactly, because not all materials meet this relatively simple hypothesis. Analytical models use

the sparse sampling of real material acquired by cameras or other optical devices, and fit the mathematical model by using the method of non-linear optimization. Addy Ngan et al.[17] used an existing high-resolution data set of a hundred isotropic materials and computed the best approximation for a variety of analytical model and got the conclusion that in the analysis of the BRDF modeling method, the whole optimization computation is very big, and the calculation result is not very stable.

Another method is to use the measured BRDF data directly in the rendering process. Data-driven method by Matusik and a sampling method by Lawrence used this approach[18, 22]. Since these BRDFs come from the measured data directly, they can preserve the subtleties of the data that may be lost in an analytical model and get very realistic results. The main disadvantage of Matusik et al.'s data-driven model is that each BRDF is stored separately as a tabulated data structure which requires about 17 MB memory. There are also some models combined empirical model or data based analytical model with the surface structure of materials. Marschner[9] and Sadeghi[10] combined the measured BRDF data with the surface structure to build a BRDF model to describe cloth or finished wood. These methods can simulate the appearance of complex highlights and color shifts which cannot be fully handled by pure analytical models. However, the main disadvantage of these models is the need to express the structure of the materials which leads to the description of a specific kind of materials. All the analytical methods use the exact above procedure to represent the material reflection properties and in the process part of the reflection information gets lost.

In recent years, BRDF modeling based machine learning also appeared. Dong Yue[14] proposed manifold bootstrapping for obtaining high-resolution reflectance from sparse captured data to build the BRDF model. Gargan and Neelamkavil[24] presented a model which uses neural networks for approximating reflectance functions. Kurt and Cinsdikici[15] introduced a new BRDF model which uses SOMs and MANs to represent measured BRDF data.

The Gaussian process in machine learning is the generalization of a probability distribution (which describes a finite-dimensional random variables) to functions[16, 20]. It does not give a definite function, but a combination of functions with different weights which can describe more complex information[16]. In addition, computations of Gaussian process required for inference and learning is relatively easy. Over the last decade, theoretical and practical developments have made Gaussian processes a serious competitor for real supervised learning, especially for high dimension and non-linear data. However, we haven't seen anyone apply Gaussian process into material reflection properties modeling in our research. So, in this paper, we introduce Gaussian process model and do the experiments based on Matusik et al.'s measured BRDFs. By using Gaussian process to predict, measurement times of BRDF data can be reduced which is time consuming and causes harm to cultural antiques. Also it can get a good rendering result with small difference compare to the real scene.

### 3 Representing BRDFs

#### 3.1 Gaussian Process Model

Gaussian process[16] defines a probability distribution (which describes a finite-dimensional random variables) to different functions. The Gaussian process model of BRDF is completely defined by the mean function and covariance function, as shown in formula (2).

$$f(\mathbf{x}) \sim GP(m(\mathbf{x}), k(\mathbf{x}, \mathbf{x}')) \quad (2)$$

The mean function  $m(\mathbf{x})$  and covariance function  $k(\mathbf{x}, \mathbf{x}')$  of a process  $f(\mathbf{x})$  is defined as:

$$m(\mathbf{x}) = E[f(\mathbf{x})] \quad (3)$$

$$k(\mathbf{x}, \mathbf{x}') = E[(f(\mathbf{x}) - m(\mathbf{x}))(f(\mathbf{x}') - m(\mathbf{x}'))] \quad (4)$$

Covariance function specifies the covariance between pairs of outputs  $f(\mathbf{x}_i)$  and  $f(\mathbf{x}_j)$ ,

$$cov(f(\mathbf{x}_i), f(\mathbf{x}_j)) = k(\mathbf{x}_i, \mathbf{x}_j) \quad (5)$$

The experiments were carried out using different covariance function[16] (see section 4) where relatively simple rational quadratic (RQ) function is chosen as the covariance function. RQ covariance function can be seen as a scale mixture of squared exponential covariance functions (SE) with different length-scales, as shown in equation (6) and (7).

$$k_{SE}(\mathbf{x}_i, \mathbf{x}_j) = \sigma_{se}^2 \exp\left(-\frac{1}{2} \sum_{k=1}^d \frac{(x_{i,k} - x_{j,k})^2}{l_k^2}\right) \quad (6)$$

where  $l$  is the characteristic length-scale,  $\sigma_{se}^2$  is signal variance and  $k$  is the dimension of input vector.

$$k_{RQ}(\mathbf{x}_i, \mathbf{x}_j) = \left(1 + \frac{1}{2\alpha} \sum_{k=1}^d \frac{(x_{i,k} - x_{j,k})^2}{l_k^2}\right)^{-\alpha} \quad (7)$$

with  $\alpha, l > 0$  can be seen as a scale mixture of SE covariance functions with different characteristic length scales.

The problem of learning in Gaussian process is exactly the problem of finding suitable properties i.e. parameters for the RQ covariance function. This problem is described in the next two sections of the paper.

### 3.2 BRDF Prediction

Our task is to map from the input light and observation conditions (given by the angle  $\theta_{in}, \varphi_{in}, \theta_{out}, \varphi_{out}$ ) to the BRDF values. We denote the vector input as  $\mathbf{x} = (\theta_{in}, \varphi_{in}, \theta_{out}, \varphi_{out})$  and continuous output (target) as  $\mathbf{y}$ . Given a training dataset  $D$  of  $n$  observations,  $D = \{X, \mathbf{y}\} = \{(\mathbf{x}_i, \mathbf{y}_i) | i = 1, \dots, n\}$ , we want to make predictions for new input  $X_*$  that in the whole space. For a new input points  $\mathbf{x}_*$  the output BRDF  $f_*$  with the covariance matrix  $k(\mathbf{x}_*, \mathbf{x}_*)$  is,

$$f_* \sim N(0, k(\mathbf{x}_*, \mathbf{x}_*)) \quad (8)$$

if there are  $n$  training points and  $n_*$  test points,  $K(X, X_*)$  denotes the  $n \times n_*$  matrix of the covariances evaluated at all pairs of training and test data. It is similarly for other matrixes  $K(X_*, X)$ ,  $K(X, X)$  and  $K(X_*, X_*)$ .

In the process of actual measurement the observer cannot access the precise BRDF value because of the measuring conditions, but only noisy observations thereof  $\mathbf{y} = f(\theta_{in}, \theta_{out}, \varphi_{in}, \varphi_{out}) + \varepsilon = f(\mathbf{x}) + \varepsilon$ . Suppose noise follows an independent, identically distributed Gaussian distribution with zeros mean and variance  $\varepsilon \sim N(0, \sigma_n^2)$ . So the prior on the BRDF noisy observations is

$$cov(\mathbf{y}) = K(X, X) + \sigma_n^2 I \quad (9)$$

Then the joint distribution of observed BRDF value and function value is

$$\begin{bmatrix} \mathbf{y} \\ f_* \end{bmatrix} = N\left(0, \begin{bmatrix} K(X, X) + \sigma_n^2 I & K(X, X_*) \\ K(X_*, X) & K(X_*, X_*) \end{bmatrix}\right) \quad (10)$$

By conditioning the joint Gaussian prior distribution on the training data (observations), the joint prior distribution can be restricted to contain only those functions agree with the observed data points[16].

$$f_* | X, \mathbf{y}, X_* \sim N(\bar{f}_* cov(f_*)) \quad (11)$$

where,

$$\bar{f}_* \triangleq E[f_* | X, \mathbf{y}, X_*] = K(X_*, X)[K(X, X) + \sigma_n^2 I]^{-1} \mathbf{y} \quad (12)$$

$$cov(f_*) = K(X_*, X_*) - K(X_*, X)[K(X, X) + \sigma_n^2 I]^{-1} K(X, X_*) \quad (13)$$

In the formula (11), prediction mean  $\bar{f}_*$  is the output of Gaussian regress process i.e. the predicted BRDF value.

### 3.3 Parameters Training

Rusinkiewicz[19] proposed a BRDF parameterization method which changed the data from the traditional axis  $\beta = \beta(\theta_{in}, \theta_{out}, \varphi_{in}, \varphi_{out})$  into new axis  $\beta = \beta(\theta_h, \varphi_h, \theta_d, \varphi_d)$ . In the new system, isotropic BRDFs are independent of  $\varphi_h$ . The input training data reduced to a three-dimensional vector  $\mathbf{x} = (\theta_h, \theta_d, \varphi_d)$

and target  $\mathbf{y}$  is the BRDFs associated with the input  $\mathbf{x}$ . We resampled the MERL dataset as Gaussian training data and did Gaussian process training and inference in new coordinate system.

We use the method of maximizing the marginal likelihood function to determine the hyper-parameters in the covariance, mean function and likelihood function. The marginal likelihood based on output BRDFs value  $\mathbf{y}$  is  $p(\mathbf{y} | X)$ .

$$p(\mathbf{y} | X) = \int p(\mathbf{y} | f, X) p(f | X) df \quad (14)$$

In Gaussian process the prior is in line with the Gaussian distribution  $f | X \sim N(0, K)$ ,  $\theta$  is the hyper-parameters, therefore the logarithms of  $p(f | X, \theta)$  is

$$\log p(f | X, \theta) = -\frac{1}{2} f^T (K)^{-1} f - \frac{1}{2} \log |K| - \frac{n}{2} \log(2\pi) \quad (15)$$

And the likelihood is a factorized Gaussian  $\mathbf{y} | f \sim N(f, \sigma_n^2 I)$ , so

$$\log p(\mathbf{y} | X, \theta) = -\frac{1}{2} \mathbf{y}^T (K + \sigma_n^2 I)^{-1} \mathbf{y} - \frac{1}{2} \log |K + \sigma_n^2 I| - \frac{n}{2} \log(2\pi) \quad (16)$$

The partial derivatives of the marginal likelihood is

$$\begin{aligned} \frac{\partial}{\partial \theta_j} \log p(\mathbf{y} | X, \theta) &= -\frac{1}{2} \mathbf{y}^T K^{-1} \frac{\partial K}{\partial \theta_j} K^{-1} \mathbf{y} - \frac{1}{2} \text{tr} (K^{-1} \frac{\partial K}{\partial \theta_j}) \\ &= \frac{1}{2} \text{tr} ((\alpha \alpha^T - K^{-1}) \frac{\partial K}{\partial \theta_j}) \end{aligned} \quad (17)$$

where  $\alpha = K^{-1} \mathbf{y}$ , and  $\theta$  is the hyper-parameters in the covariance, i.e. length scale  $l$ ,  $\alpha$  and the noise  $\sigma_n^2$ . With maximizing the marginal likelihood function of hyper-parameters, the optimal length scale  $l$ ,  $\alpha$  and the noise  $\sigma_n^2$  are acquired. After getting the hyper-parameters, the properties of the covariance are determined and the BRDF's predicted value and its variance  $\widehat{\sigma}_{f_*}^2$  can be obtained using formula (9).

## 4 Experiment and Result Evaluation

In order to verify the feasibility of Gaussian process in BRDF prediction, we use the current light model to generate discrete BRDF data, and use GP to fit these examples. Figure 1 shows the BRDF distribution of five different models (empirical model: Phong[3], Blinn Phong[8], anisotropic model Bank Phong[23] and physically-based model: Cook Torrance[7], Blinn[8]) under the fixed light direction and different observation directions. The top row is the ground truth (generated by current models) and the bottom row is the predicted results by GP with the training data shown by red stars.

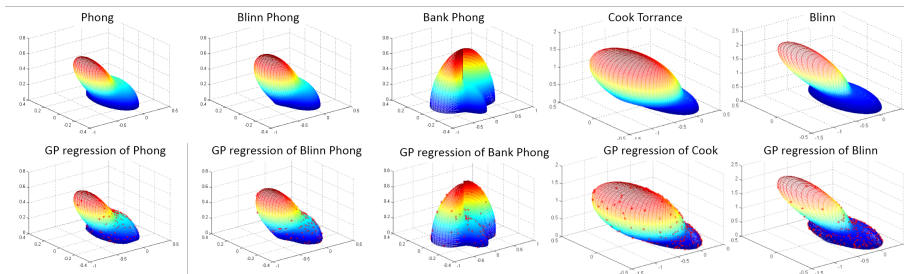


**Fig. 1.** Comparison between existing models and the GP regression

To evaluate the BRDF value predicted by Gaussian process quantificationally, we use mean absolute error (MAE) and mean-square error (MSE) to measure the difference between predicted BRDF value and the ground-truth,

$$\sigma_{MAE} = \frac{1}{N} \sum_{i=1}^N |\bar{\mathbf{y}}(i) - \mathbf{y}(i)| \quad (18)$$

$$\sigma_{MSE} = \frac{1}{N} \sum_{i=1}^N (\bar{\mathbf{y}}(i) - \mathbf{y}(i))^2 \quad (19)$$

**Table 1.** Gaussian process prediction error of current models

|     | Phong    | Bank Phong | Blinn Phong | Ward     | Blinn    |
|-----|----------|------------|-------------|----------|----------|
| MAE | 1.72E-04 | 0.0021     | 8.99E-04    | 1.18E-04 | 4.31E-04 |
| MSE | 0.0017   | 0.0167     | 0.0034      | 0.0037   | 0.0038   |

We can see from Figure 1 and Table 1 that GP can get good fitting and prediction for the current model. Hence, a conclusion can be made that Gaussian process can be used for better BRDF prediction of real materials.

For real materials, we test Gaussian process on MERL[18] material database to test the prediction performance of GP. The measurements of Matusik et al.[18] provide a dense (90\*90\*180 for values) sampling of many isotropic BRDFs. Every material is described by 1458000 BRDFs in tabular form. It acquires good rendering results compared favorably with real materials, but the main drawback of these representations is that their size is too large. We also made experiments on the sampling rate and error relationships using part of BRDF data to do inference, as shown in Figure 2. With the increase of sampling rate, the prediction error reduces greatly. Also the corresponding training time will increase significantly. So for each material, we choose 2.58% (37616 for values) of BRDF data as the training data, use Gaussian process to learn the relationship between BRDFs of different angles, and infer the GP model.

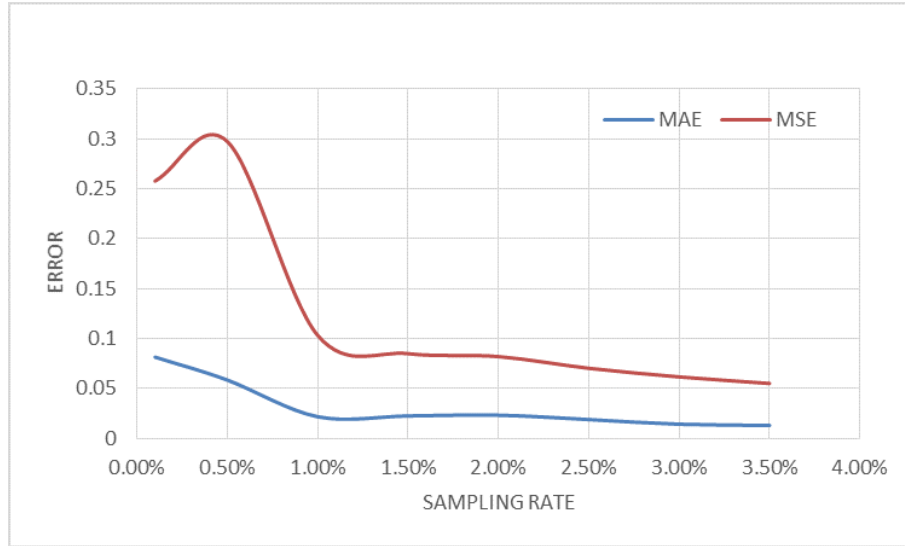


**Fig. 2.** The prediction error reduces as the increase of sampling rate.



The ground truth (rendered using MERL BRDF data directly) and the GP model result of the material “Cherry-235” is shown by Disney’s BRDF explorer[21] in Figure 3. A Terra Cotta Warriors model are lighted by a point light (a) and an environment map (b). The top row is the MERL rendering result and the bottom row shows the result of the proposed work. From left to right, the first column is the rendering results by point lighting, the second column is rendering results based on image lighting and the third is the image slices.[21]

(a)Point light                      (b)Image based light                      (c) $\varphi_d = 90$  Image slice

**Fig. 3.** The MERL and Gaussian process prediction rendering results of “Cherry-235”. (By using only 2.58% of the MERL datasets, the proposed work attains almost the same rendering performance.)

$\varphi_d = 90$  image slice is a method to visualize the BRDF features proposed by Brent Burley et al[21]. All of the interesting features of materials are visible in the  $\varphi_d = 90$  image. By comparing the BRDF image slices, we can see the difference between predicted and true BRDF value intuitively. Figure 4 shows the schematic view of the image slice and six image slices of materials. The materials include painting, rubber, plastic, fabric, etc. and use RQ as the Gaussian process’s covariance.

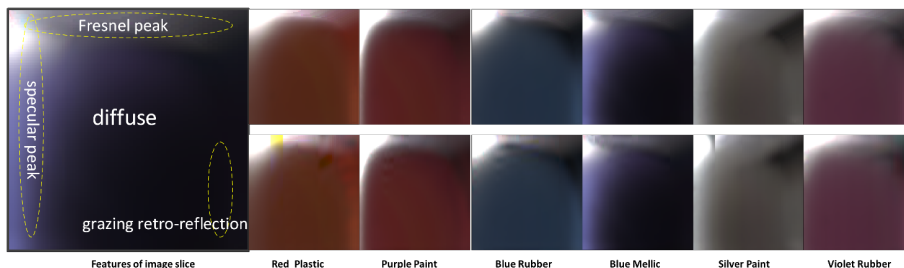


**Fig. 4.** The BRDF image slices. All of the interesting features of materials such as diffuse, specular Fresnel peak and retro-reflection is visible in the  $\varphi_d = 90$  image. The figure shows the different between ground truth and predicted values of six materials.

Figure 3(c) and Figure 4 shows that usually the upper left corner of the slice is the difference between the ground truth and the predicted results, which is near to the specular and Fresnel peak. One reason for such a case is that, BRDF changes dramatically near the specular and Fresnel peak but in the proposed work we choose the same sampling interval for different angles. Increasing the density of sampling near the angles of specular and Fresnel can modify this problem, but as a drawback this will increase the computational complexity of the covariance matrix.

The rendering results of the proposed work are shown in the Figure 5, where the Gaussian process can get good results under both point lighting and image lighting. It is difficult to distinguish the difference between ground truth and GP regression results with the naked eye. So we calculate the pixel difference value between them by using  $1-b/a$  ( $a$ ,  $b$  are the pixel values of two point light image, respectively). The difference of figure 5(a) and figure 5(b) is much smaller than the difference of point light image, we did not show them) and show the distribution in Fig.5 (e). As Fig.5 (e) shows, the difference is under 5% of true BRDF rendering value.

As the visual effect of the rendering results depends on people’s psychological perception, there is still no unified standard to measure. Since PSNR is an objective criterion for evaluation of image, we use peak signal to noise ratio (PSNR) to evaluate the image of object model rendered by predicted BRDF and the ground truth.

$$PSNR = 10 * \log \left( \frac{(2^n - 1)^2}{MSE} \right) \quad (20)$$

where,  $MSE$  is the mean square error between the original image and process images.

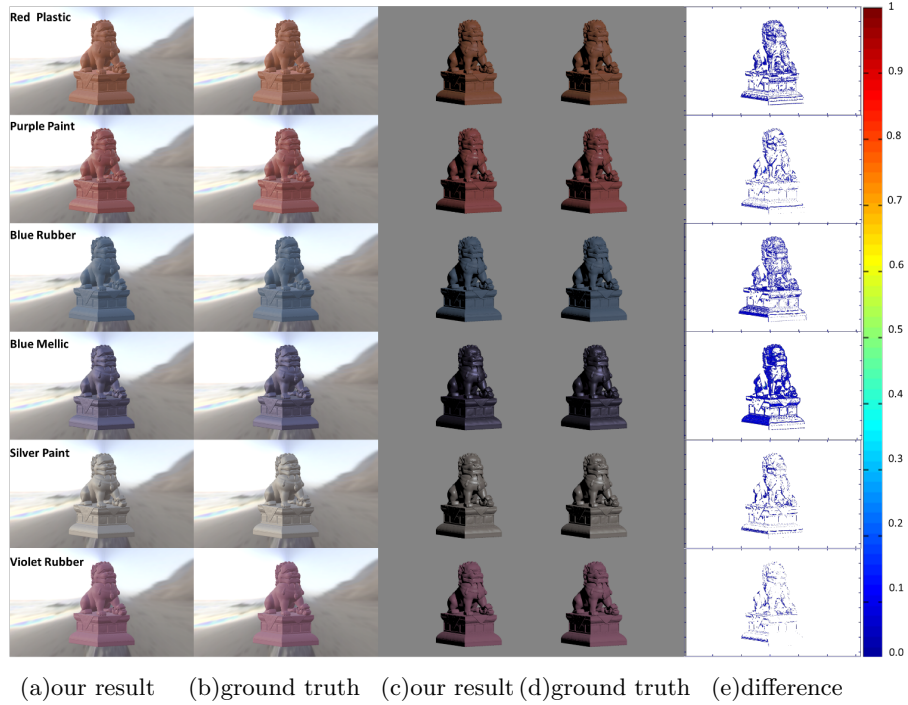


**Fig. 5.** GP regression results of 6 different materials (red plastic, purple paint, blue rubber, blue melic, silver paint, violet rubber) under the image based light (a) (b) and point light (c) (d). (e) Pixel difference value between ground truth and proposed work.

Table 2 gives the different error analysis of these 6 materials. The representations error of these 6 materials with RQ covariance is very small and our PSNR is much higher than other methods (Phong: 32.09, Blinn-Phong: 30.97, Cook-Torrance: 32.98, Murat Kurt: 52.12)[15].

Covariance functions are used to describe the relationship between different outputs. Also we experimented using different covariance function and their combination[16](formula 6,7 and 22), this is the reason that we chose the rational quadratic (RQ) function with little error to be the covariance function in section 3.1.

Matern class function (Matern)

**Table 2.** Gaussian process prediction error of different materials

|             | red plastic | purple paint | blue rubber | blue melic | silver paint | violet rubber |
|-------------|-------------|--------------|-------------|------------|--------------|---------------|
| <i>MAE</i>  | 0.0144      | 0.0048       | 0.0049      | 0.0028     | 0.0124       | 0.0054        |
| <i>MSE</i>  | 0.0375      | 0.0248       | 0.0259      | 0.0212     | 0.0345       | 0.0253        |
| <i>PSNR</i> | 62.3924     | 64.1940      | 63.9993     | 64.8764    | 62.7547      | 64.0961       |

$$k_\nu(\mathbf{x}_i, \mathbf{x}_j) = \sigma_m^2 \frac{2^{1-\nu}}{\Gamma(\nu)} (\sqrt{2\nu r})^\nu K_\nu(\sqrt{2\nu r}) \quad (21)$$

where,  $r = \left( \sum_{k=1}^d \frac{(x_{i,k} - x_{j,k})^2}{l_k^2} \right)^{\frac{1}{2}}$ .  $\nu$  is used to control the roughness of process, and  $K_\nu$  is the modified Bessel function.

**Table 3.** Gaussian process prediction error with different covariance

| <i>Error</i>   | <b>Gaussian Process Prediction Error</b> |         |         |           |                |         |
|----------------|--|---------|---------|-----------|----------------|---------|
|                | RQ                                       | SE      | Matern  | Matern+SE | Matern+RQ      | RQ+SE   |
| $\sigma_{MAE}$ | 0.0134                                   | 0.0156  | 0.0122  | 0.0800    | 0.0187         | 0.0205  |
| $\sigma_{MSE}$ | 0.0830                                   | 0.0875  | 0.0837  | 0.4527    | 0.0992         | 0.1078  |
| <i>PSNR</i>    | <b>54.4767</b>                           | 50.2725 | 52.6951 | 36.1594   | <b>57.2624</b> | 52.9558 |

## 5 Future Work

In the proposed work, Gaussian process is used to predict real BRDFs. The experiments show that the error of prediction is small, the peak signal to noise ratio of the rendering image is high and the results can satisfy the demand of practical application.

Using Gaussian process based on Bayesian method can not only achieve accurate prediction but also reduce the complexity and time consumption of BRDF measurement procedure. However, a significant problem with Gaussian process used in BRDF prediction is that for large data processing problems both storing the Gram matrix and solving the associated linear systems are prohibitive on modern workstations. Also, the training process of GP is time-consuming and the learning process is done offline now. With the ascension of computer hardware technology and improvement of the algorithm, real-time calculation is promising to realize.

In this paper, we only considered the isotropic homogeneous materials whose reflection properties is not supposed to change with spatial location. As a four dimensional function, although BRDF describes the illumination properties of

different view and light direction on the materials surface, it can only describes the reflection law of homogeneous material. For some uneven material surface of cultural relics, there will be self-occlusion, self-shadow, occlusion and other complicated visual effects. BTF (Bidirectional texture function) can not only capture the changes in light properties along with the light and view direction but also capture the sampling location. In future, we will focus on the research of non-homogeneous relic's material and BTF representations.

**Acknowledgement.** This work was supported by the National Key Technology Support Program under Grant 2012BAH64F01 and 2013BAH48F01 and National Natural Science Foundation of China 61370134. The authors would like to thank Wojciech Matusik et al.[14] for using their measured BRDF data.

## References

1. Nicodemus, F.E.: Geometrical considerations and nomenclature for reflectance. US Department of Commerce, National Bureau of Standards, Washington, D. C. (1977)
2. Matusik, W., et al.: Efficient isotropic BRDF measurement. Eurographics Association, Proceedings of the 14th Eurographics workshop on Rendering (2003)
3. Phong, B.T.: Illumination for computer generated pictures. *Communications of the ACM* **18** (1975) 311–317
4. Ward, G.J.: Measuring and modeling anisotropic reflection. *ACM SIGGRAPH Computer Graphics* **26** (1992) 265–272
5. Ashikhmin, M., Shirley, P.: An anisotropic phong BRDF model. *J. of graphics tools* **5** (2000) 25–32
6. Torrance, K.E., Sparrow, E.M.: Theory for off-specular reflection from roughened surfaces. *JOSA* **57** (1967) 1105–1112
7. Cook, R.L., Torrance, K.E.: A reflectance model for computer graphics. *ACM Transactions on Graphics (TOG)* **1** (1982) 7–24
8. Blinn, J.F.: Models of light reflection for computer synthesized pictures. *ACM SIGGRAPH Computer Graphics* **11** (1977) 192–198
9. Marschner, S.R., et al.: Measuring and modeling the appearance of finished wood. *ACM Transactions on Graphics (TOG)* **24** (2005) 727–734
10. Sadeghi, I., et al.: A practical microcylinder appearance model for cloth rendering. *ACM Transactions on Graphics (TOG)* **32** (2013) 14
11. Ngan, A., Durand, F., Matusik, W.: Experimental analysis of BRDF models. Proceedings of the Sixteenth Eurographics conference on Rendering Techniques, Eurographics Association (2005)
12. Lafortune, E.P.F., et al.: Non-linear approximation of reflectance functions. Proceedings of the Sixteenth Eurographics conference on Rendering Techniques, Eurographics Association (1997)
13. He, X.D., et al.: A comprehensive physical model for light reflection. *ACM SIGGRAPH Computer Graphics* **25** (1991) 175–186
14. Dong, Y., et al.: Manifold bootstrapping for SVBRDF capture. *ACM Transactions on Graphics (TOG)* **29** (2010) 98
15. Kurt, M., Cinsdikici, M.G.: Representing BRDFs using SOMs and MANs. *ACM SIGGRAPH Computer Graphics* **42** (2008) 2
16. Rasmussen, C.E.: Gaussian processes for machine learning. the MIT Press (2006)

17. Ngan, A., Durand, F., Matusik, W.: Experimental analysis of BRDF models. Eurographics Association, Proceedings of the Sixteenth Eurographics conference on Rendering Techniques (2005)
18. Matusik, W.: A data-driven reflectance model. University of North Carolina, Chapel Hill (2003)
19. Rusinkiewicz, S.M.: A new change of variables for efficient BRDF representation. Rendering techniques 98. Springer Vienna (1998)
20. Vanhatalo, J., et al.: GPstuff: Bayesian modeling with Gaussian processes. J. of Machine Learning Research **14** (2013) 1175–1179
21. Burley, B., Studios, W.D.A.: Physically-Based Shading at Disney. Practical Physically-Based Shading in Film and Game Production, SIGGRAPH (2012)
22. Lawrence, J., Rusinkiewicz, S., Ramamoorthi, R.: Efficient BRDF importance sampling using a factored representation. ACM Transactions on Graphics (TOG) **23** (2004) 496–505
23. Nicodemus, F.E.: Directional reflectance and emissivity of an opaque surface. Applied Optics **4** (1965) 767–773
24. Gargan, D., Neelamkavil, F.: Approximating reflectance functions using neural networks. Rendering Techniques' 98, Springer Vienna (1998)
25. Ghosh, A., et al.: A basis illumination approach to BRDF measurement. International journal of computer vision **90** (2010) 183–197
26. Zupancic, B., Soler, C.: Sparse BRDF approximation using compressive sensing. SIGGRAPH Asia 2013 Posters, ACM (2013)